

Marquette University  
**e-Publications@Marquette**

---

Chemistry Faculty Research and Publications

Chemistry, Department of

---

4-9-2009

# Material properties of nanoclay PVC composites

Walid Awad

Marquette University, [walid.awad@marquette.edu](mailto:walid.awad@marquette.edu)

Gunter Beyer

Kabelwerk Eupen

Daphne Benderly

Elementis Specialties

Wouter L. Ijdo

Elementis Specialties

Ponusa Songtipya

Pennsylvania State University - Main Campus

*See next page for additional authors*

---

Accepted version. *Polymer*, Vol. 50, No. 8 (April 9,2009): 1857-1867. DOI. © 2009 Elsevier B.V.  
Used with permission.

---

**Authors**

Walid Awad, Gunter Beyer, Daphne Benderly, Wouter L. Ijdo, Ponusa Songtipya, Maria del Mar Jimenez-Gasco, Evangelos Manias, and Charles A. Wilkie

Marquette University

**e-Publications@Marquette**

***Chemistry Faculty Research and Publications/College of Arts and Science***

***This paper is NOT THE PUBLISHED VERSION; but the author's final, peer-reviewed manuscript.***

The published version may be accessed by following the link in the citation below.

*Polymer*, Vol. 50, No. 8 (April, 2009): 1857-1867. [DOI](#). This article is © Elsevier and permission has been granted for this version to appear in [e-Publications@Marquette](#). Elsevier does not grant permission for this article to be further copied/distributed or hosted elsewhere without the express permission from Elsevier.

# Material Properties of Nanoclay PVC Composites

**Walid H. Awad**

Department of Chemistry and Fire Retardant Research Facility, Marquette University, Milwaukee, WI

**Günter Beyer**

Kabelwerk Eupen, Belgium

**Daphne Benderly**

Elementis Specialties, Hightstown, NJ

**Wouter L. Ijdo**

Elementis Specialties, Hightstown, NJ

**Ponusa Songtipya**

Penn State University, Polymer Nanostructures Lab—CSPS and Materials Science and Engineering Department, University Park, PA

Penn State University, Plant Pathology Department, University Park, PA

**Maria del Mar Jimenez-Gasco**

Penn State University, Plant Pathology Department, University Park, PA

## E. Manias

Penn State University, Polymer Nanostructures Lab—CSPS and Materials Science and Engineering Department, University Park, PA

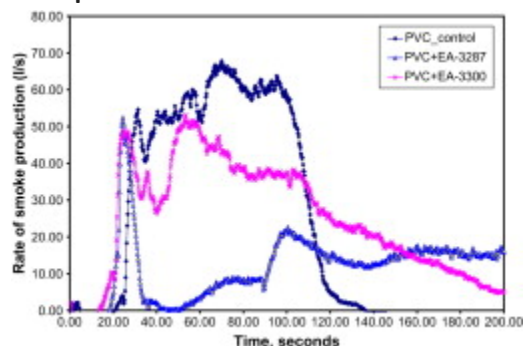
## Charles A. Wilkie

Department of Chemistry and Fire Retardant Research Facility, Marquette University, Milwaukee, WI

## Abstract

Nanocomposites of poly(vinyl chloride) have been prepared using both hectorite- and bentonite-based organically-modified clays. The organic modification used is tallow-triethanol-ammonium ion. The morphology of the systems was investigated using X-ray diffraction and transmission electron microscopy and these systems show that true nanocomposites, both intercalated and exfoliated systems, are produced. The mechanical properties have been evaluated and the modulus increases upon nanocomposite formation without a significant decrease in tensile strength or elongation at break. Thermal analysis studies using thermogravimetric analysis, differential scanning calorimetry, and dynamic mechanical analysis were conducted. Thermal stability of the PVC systems was assessed using a standard thermal process evaluating the evolution of hydrogen chloride and by color development through the yellowness index. Cone calorimetry was used to measure the fire properties and especially to evaluate smoke evolution. The addition of an appropriately-modified bentonite or hectorite nanoclay leads to both a reduction in the total smoke that is evolved, and an increase in the length of time over which smoke is evolved. Along with this, a reduction in the peak heat release rate is seen. It is likely that the presence of the clay in some way interferes with the cyclization of the conjugated system formed upon HCl loss.

## Graphical abstract



## Keywords

PVC nanocomposites; Fire retardancy; Thermal stability

## 1. Introduction

The past decade has seen a great upsurge in research on polymer–clay nanocomposites, because these materials can offer enhanced fire, mechanical and barrier properties compared to polymer composites containing traditional fillers. Work has been conducted on a wide variety of polymers, including

thermoplastics, such as styrenics, polyolefins, etc. and thermosetting materials, such as epoxy resins and phenolics.

Despite this recent proliferation of nanoclays as additives for polymers in academic research and, to a lesser extent, in industrial practice, high performing clay-reinforced nanocomposites based on poly(vinyl chloride) (PVC) have remained elusive. The main challenge with these systems relates to the common ammonium-based organic treatments of the clays, which typically yield an amine during the processing of the nanocomposite, and this amine can accelerate the degradation of the PVC. In order to avoid this degradation, one must use a much less-basic amine, perhaps an imidazolium<sup>[1], [2]</sup>, or some other nano-dimensional material such as a layered double hydroxide, LDH, might be used. There is a recent report<sup>[3]</sup> of a PVC–LDH composite which has much better thermal stability than does PVC, probably because the hydroxides can absorb the HCl as it is evolved. Nonetheless, the HCl is still evolved with concomitant degradation of the PVC and this has not been examined.

Efforts to obtain PVC–montmorillonite nanocomposites have employed melt blending<sup>[4], [5], [6], [7], [8], [9], [10], [11], [12], [13]</sup>, solution blending<sup>[14]</sup> and polymerization<sup>[15]</sup>, using either the pristine sodium clay or organically-modified clays. With melt blending, degradation of the PVC typically occurs quite rapidly, accompanied by strong discoloration. When organically-modified layered-silicate clays are used, in general good dispersion of the clay in the polymer can be achieved, normally as intercalated systems; in contrast, when pristine alkaline clays are used, the dispersion is not as good. Where mechanical properties have been examined, they appear to be improved by the addition of a small amount of clay, but are decreased with larger amounts of the clay<sup>[7], [9]</sup>. A study using X-ray photoelectron spectroscopy on PVC–clay (nano)composites has found that the presence of the clay seems to retard the chain-stripping process of degradation and that enhanced char formation is observed<sup>[16]</sup>.

The recent introduction of a new nanoclay, which contains a tallow-triethanol-ammonium cation, has motivated us to revisit this material to see if there is an advantage in making PVC nanocomposites. The nanocomposites have been evaluated using the standard thermal stability test for PVC, as well as by thermogravimetric analysis (TGA), differential scanning calorimetry (DSC), dynamic mechanical analysis (DMA), tensile mechanical measurements, rheometry and cone calorimetry. Nanocomposite formation was evaluated using X-ray diffraction (XRD) and transmission electron microscopy (TEM).

## 2. Experimental

### 2.1. Materials

Semi-rigid PVC 9209 compound supplied by Georgia Gulf was used. The two nanoclays used are developmental additives based on hectorite (EA-3300) (CEC = 75 meq/100 g) and bentonite (EA-3287) clay (CEC = 98 meq/100 g) and are manufactured by Elementis Specialties; the quaternary ammonium used as an organic modifier for the clays is tallow-triethanol-ammonium (TTA). The stoichiometric amount of the surfactant was used in the preparation of these organically-modified clays. Other fillers evaluated are superfine talc (Nytal 400, R.T. Vanderbilt), calcium carbonate (Omycarb 4, Omya), and kaolin clay (Huber 80, Huber Engineered Materials). DIDP (di-isodecyl phthalate) plasticizer was obtained from W.N. Stevenson Co. Propylene carbonate dispersing agent was obtained from Sigma Aldrich.

## 2.2. Composite preparation

Two sets of composites were prepared. In the first set, PVC was compounded with the various fillers. The PVC and filler were mixed at 180 °C and 50 rpm for 8 min in a Brabender mixing chamber. The filler content was 3 wt% for the organo-clays, while the other fillers were used at a loading level of 2 wt%, to give a similar inorganic loading level. The compounded material was granulated and injection molded. In the second set of composites, DIDP plasticizer was added as well. Two mixing methods were used for these composites, a direct mix and a pre-gel method. In the direct mix method (mixing order 1, **mo1**), all the components were added directly to the Brabender mixer. In the pre-gel method (mixing order 2, **mo2**), nanoclay was first mixed with DIDP under high shear. Mixing was conducted in a Dispermat blender, using a 40 mm blade. The nanoclay is slowly added to the DIDP and then mixed for 5 min at 4000 rpm. This mixture was subsequently compounded into PVC using a Brabender mixer. Propylene carbonate (PC) was added to some of the PVC formulations. PC is a well-known polar activator, used for improving nanoclay dispersion in organic solvents<sup>[18]</sup>. Based on previous optimization testing, the level of PC in the nanocomposites was set at 21% by weight of the nanoclay loading level. For composites prepared using the pre-gel method, the dispersant was added with the nanoclay to the DIDP.

## 2.3. Characterization

The evolution of hydrogen chloride from the PVC composite was evaluated at 200 °C according to the EN 60811-3-2 protocol. According to this protocol, the time to degradation is taken as the time at which there is a visible change in a piece of Congo Red pH paper held in the effluent stream. Samples were aged in a conventional laboratory oven with ventilation for seven days at 80 °C according to EN 60811-1-2. The measurement of tensile strength elongation, and modulus followed the EN 60811-1-1 and IEC 60811-1-1 protocols using a Tensometer from Alpha Technologies and a speed of testing (relative rate of motion of the grips) of 250 mm/min, unless otherwise noted. Additional tensile testing was done on an Instron 5800 tensile tester following the ASTM D638-08 protocol, with small type-IV (dogbone) specimens and a 50 mm/min speed of testing.

The thermal stability of the composites was evaluated by thermogravimetric analysis (TGA), on a TA Instruments TGA 2950, operated in air at a rate of 10 °C/min. The glass transition temperature ( $T_g$ ) was evaluated using differential scanning calorimetry (DSC) using a TA Instruments DSC 2010, operated in nitrogen at a rate of 10 °C/min. Dynamic mechanical analysis in torsion mode was conducted using a TA Instruments AR 1000 rheometer. The storage modulus, loss modulus and tan delta were determined. The test was performed using a temperature range of 30–90 °C, at a frequency of 1 Hz. The linear viscoelastic region was first evaluated to determine the appropriate test conditions. The glass transition temperature ( $T_g$ ) is taken as the peak of the  $G''$  curve.

X-ray diffraction data was obtained using a Rigaku MiniflexII diffractometer equipped with Cu-K $\alpha$  source ( $\lambda = 1.5404 \text{ \AA}$ ). It was operated at 50 kV and 20 mA and scans were obtained in a  $2\theta$  range from 2° to 10°, with a 0.1° step size. Bright field transmission electron microscope (TEM) images of the samples were obtained with a JEOL 1200 EXII operated with an accelerating voltage of 80 kV, and equipped with a Tietz F224 digital camera. Ultrathin sections (70–100 nm) of the nanocomposites were obtained with an ultramicrotome (Leica Ultracut UCT) equipped with a diamond knife. The sections were transferred to carbon-coated copper grids (200-mesh, with a Lacey support film). No heavy metal staining of sections prior to imaging was done, since the contrast between the fillers and the polymer matrix was sufficient. Atomic force microscope (AFM) images of organically-modified clays were obtained using a

Digital Instruments MultiMode SPM. A dilute (0.01%) organoclay solution was first delaminated in toluene using propylene carbonate as a dispersing agent, and then sonicated. A drop was pipetted onto a mica substrate, which was glued to a metal AFM stub, and the toluene allowed to dry. The samples were analyzed using tapping mode. Height, phase and amplitude images were obtained from multiple areas of the same sample. Color development, also in the presence of fillers and additives, was quantified through the yellowness index (YI), measured in a Datacolor instrument following the tristimulus definition as per the ASTM E313 protocol. Digital photos of the specimens, before and after thermal aging, were obtained by a Ricoh color scanner (Aficio MP C3500) and true color and white balance correction were done by concurrent imaging of standardized typographic RGB color scales.

Cone calorimetry measurements were performed on an Atlas CONE2 instrument, according to ASTM E 1354 at an incident flux of 50 kW/m<sup>2</sup> using a cone shaped heater. The spark was continuous until the sample ignited and the exhaust flow rate was 24 L/s. The specimens for cone calorimetry were prepared by the compression molding of the granulated sample (about 30 g) into 3 mm × 100 mm × 100 mm plaques. Typically, results from cone calorimetry are reproducible to within ±10%.

### 3. Results and discussions

#### 3.1. Thermal stability

The degradation of PVC has been studied for many years and there is some consensus regarding the course of degradation. It proceeds by a chain-stripping process, which eliminates HCl with the concomitant formation of alternating double bonds along the polymer chain; this reaction commences at about 190 °C<sup>[17]</sup>. The material that contains the double bonds then undergoes cyclization reactions which lead to a large amount of smoke upon burning. In order to evaluate the thermal stability of PVC compounds, a sample is typically heated to a certain temperature and the time for HCl evolution is measured. The results of this evaluation are given in [Table 1](#), [Table 2](#). Several controls have been used in this study, including PVC with no additional filler, and PVC with only the quaternary ammonium ion; two other inorganic materials were also used, kaolin and talc, which have comparable structures as the hectorite/bentonite clays but do not contain organic modifiers.

Table 1. Thermal stability of PVC with various additives.

Compound	Time to degradation (min)		
	After processing on a rolling mill	After pressing at 180 °C, 300 bar	After aging at 80 °C, 7 days
PVC	27	22	20
PVC + talc	26	21	21
PVC + kaolin	25	20	19
PVC + hectorite <sup>a</sup>	23	18	18
PVC + bentonite <sup>a</sup>	17	13	13
PVC + organic modifier <sup>a</sup>	16	10	10

<sup>a</sup> The organic modifier is triethanol-tallow-ammonium, and is used for the organic modification for both the hectorite and the bentonite nanoclays.

Table 2. Effect of mixing order and additives on the thermal stability of plasticized PVC.

Compound	Time to degradation (min)		
	After processing on a rolling mill	After pressing at 180 °C, 300 bar	After aging at 80 °C, 7 days
PVC + plasticizer + dispersant	40	34	25
<b>Mix order 1</b>			
PVC + plasticizer + bentonite	19	16	14
PVC + plasticizer + bentonite + dispersant	18	17	15
PVC + plasticizer + hectorite	30	21	21
PVC + plasticizer + hectorite + dispersant	25	22	22
<b>Mix order 2</b>			
PVC + plasticizer + bentonite	19	17	14
PVC + plasticizer + bentonite + dispersant	18	16	16
PVC + plasticizer + hectorite	24	22	21
PVC + plasticizer + hectorite + dispersant	31	28	24

The greatest change in thermal stability occurs when only the ammonium organic modifier is added to the PVC ([Table 1](#)). This is not surprising since an amine group, which is potentially generated through a Hoffmann degradation of the quaternary ammonium, can promote degradation of PVC. The addition of either talc or kaolin has little effect on the time to degradation, while the addition of organically-modified hectorite has a greater effect ([Table 1](#)). The addition of organically-modified bentonite has an even greater effect on thermal stability; this is possibly due to the better dispersion of the bentonite, as will be shown later, which results in higher exposure of the PVC matrix to the organo-modifications on the clay. As expected, the time to degradation decreases after further processing or thermal aging. For each material, the times to degradation are quite similar for systems that have been further processed (hot-pressed at 180 °C and 300 bar) and those that were thermally aged (at 80 °C for 7 days).

Two mixing methods were used for the PVC/DIDP composites. In the direct mix method (mixing order 1, **mo1**), all components were added directly to the Brabender mixer. In the pre-gel method (mixing order 2, **mo2**), organically-modified clay was first mixed with the DIDP plasticizer and subsequently melt processed with PVC. One may also use a dispersant (propylene carbonate) to assist in organoclay delamination<sup>[18]</sup>. Thermal stability results for composites prepared by both methods are shown in [Table 2](#). When plasticizer is added to the polymer, the thermal stability increases relative to the initial PVC,



further addition of hectorite causes only a small decrease in thermal stability, whereas a larger decrease is seen for bentonite fillers.

The addition of the (propylene carbonate) dispersant to PVC/DIDP without organoclay enhances the thermal stability; while the thermal stability is either decreased (uncompounded material) or little changed (processed or aged material) when both dispersant and nanoclay are added using the direct mix method. Similar trends are observed upon both further processing and thermal aging, with better thermal stability obtained with hectorite nanoclay, as compared to bentonite nanoclay.

### 3.2. Yellowness index

The addition of any of the fillers discussed shifts the color of PVC, which was measured spectroscopically using a Datascolor instrument. The PVC color can be described by either the color coordinates  $L^*a^*b^*$ , or by the yellowness index (YI). A shift in color can be calculated as  $\Delta E$  (square root of the sum of the squares of the changes in  $L^*$ ,  $a^*$  or  $b^*$ ), or as the shift in yellowness index ( $\Delta YI$ ).

As PVC degrades upon aging, yellowing occurs. The extent of the discoloration was characterized, and these results are provided in [Table 3](#), [Table 4](#) for composites without and with plasticizer, respectively. Values are not provided for the PVC with the addition of TETQ, as the mixing was very inhomogeneous. A complete set of color images of all samples is included in the [Supporting material](#).

Table 3. Yellowness index (YI) values and photographs for PVC and its composites with different fillers, before (as processed) and after thermal aging (7 days at 80 °C).

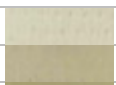
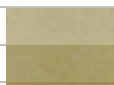
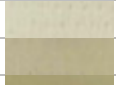
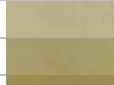
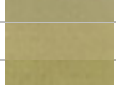
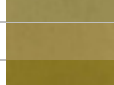


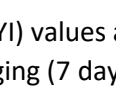
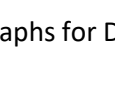

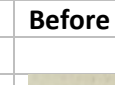


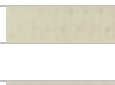

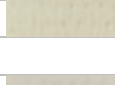
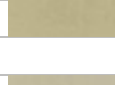
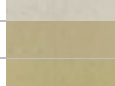
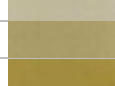
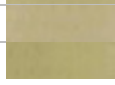

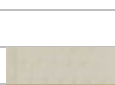
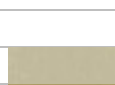
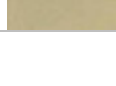
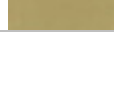




Additive type	Before aging		After aging		$\Delta YI$
		YI		YI	
PVC (no additive)		25.3		34.5	9.2
Talc		36.8		46.0	9.2
Kaolin		45.4		56.8	11.4
Hectorite		56.6		69.8	13.2
Bentonite		60.9		82.8	21.9
Organic modifier (TETQ)		N/A		N/A	

Table 4. Yellowness index (YI) values and photographs for DIDP-plasticized PVC and its nanocomposites, before and after thermal aging (7 days at 80 °C).

Compound	Before aging		After aging		$\Delta YI$
		YI		YI	
PVC (no additives)		25.3		34.5	9.2
<b>PVC + plasticizer</b>		14.0		22.5	8.5
PVC + plasticizer + hectorite ( <b>mo1</b> )		37.9		49.7	11.8
PVC + plasticizer + bentonite ( <b>mo1</b> )		46.8		79.5	32.7
PVC + plasticizer + hectorite ( <b>mo2</b> )		39.4		49.3	9.9
PVC + plasticizer + bentonite ( <b>mo2</b> )		53.0		80.4	27.4
<b>PVC + plasticizer + dispersant</b>		18.4		24.1	5.7
PVC + plasticizer + dispersant + hectorite ( <b>mo1</b> )		38.2		53.1	14.9

PVC + plasticizer + dispersant + bentonite (mo1)		46.9		78.9	32.0
PVC + plasticizer + dispersant + hectorite (mo2)		41.7		46.6	4.9
PVC + plasticizer + dispersant + bentonite (mo2)		53.5		77.0	23.5

**mo1:** mixing order 1, one-shot direct compounding.

**mo2:** mixing order 2, pre-gel of organoclay in DIDP with subsequent addition to PV

The color of PVC, without fillers, becomes yellower after aging due to degradation. PVC composites with either talc, kaolin or hectorite exhibit a similar color shift upon aging, while the addition of bentonite causes a greater color shift upon aging, and thus more degradation. This observation agrees with the thermal stability results presented in [Table 1](#).

When the plasticizer is present, the PVC color is less yellow than the PVC without plasticizer ([Table 4](#)), but a similar shift in color upon aging occurs. The addition of the dispersant slightly yellows the PVC, and reduces the extent of degradation upon aging.

Formulation with hectorite organoclay yields a composite with less color shift from the PVC base, as compared to bentonite organoclay. In addition, hectorite organoclay causes less yellowing upon aging, as compared to bentonite organoclay. These results are in agreement with the thermal stability results presented in [Table 2](#). The mixing order has a relatively small effect on color development in composites without dispersant; for composites containing dispersant, less color shift is seen with mixing order 2 (pre-gel method).

### 3.3. Mechanical properties

Room temperature mechanical properties were evaluated using a tensile tester, while the temperature dependence of the modulus was also evaluated by torsion-mode dynamic mechanical analysis. The various tensile moduli are given in [Table 5](#) for PVC/filler composites and compared with unreinforced PVC. The addition of any clay in the PVC matrix, whether kaolin, talc, or hectorite or bentonite nanoclay, does not change markedly the yield point of the composites independent of the rate of the experiment (tensile measurements at 250 mm/min and 50 mm/min shown in [Table 5](#)). At the same time, composites with nano-level filler dispersion also show an improvement in the tensile modulus, for example hectorite and bentonite, whereas the kaolin and talc micro-fillers have a much smaller effect on the modulus. The complete set of tensile properties, including uncertainties, is provided in the [Supporting information](#).

Table 5. Mechanical properties (yield points and moduli) of PVC and PVC with additives before aging.

Compound	Yield point				Modulus		
	Tensile stress at max load <sup>a</sup> (MPa)	Tensile stress at max load <sup>b</sup> (MPa)	Tensile strain at max load <sup>a</sup> (%)	Tensile strain at max load <sup>b</sup> (%)	Young's modulus <sup>a</sup> (MPa)	Young's modulus <sup>b</sup> (MPa)	$G'$ at 30 °C (MPa)
PVC	49.4	49.3	3.7	4.9	2390	1518	899

PVC + talc	49.4	48.9	3.8	4.9	2273	1577	910
PVC + kaolin	48.2	47.4	3.6	5.0	2248	1567	988
PVC + bentonite	49.0	47.6	3.3	4.4	2797	1723	1080
PVC + hectorite	49.8	48.8	3.6	4.7	2724	1765	956

<sup>a</sup> Measured at 250 mm/min.

<sup>b</sup> Measured at 50 mm/min.

These effects are not quite as pronounced for the tensile properties when plasticizer and dispersant are added to the composites, however the trends are mostly the same (Table 6). Namely, the moduli seem to increase compared to the respective unfilled matrices (*i.e.*, plasticized PVC with or without dispersant), and this improvement is often better for the pre-gelled (mix order 2) composites. At the same time, the tensile strength (maximum tensile stress, for all systems typically near the yield point) remains the same for all composites at about 45 MPa, slightly larger than the corresponding unfilled matrix (the plasticized PVC has a tensile strength of about 43 MPa; Table 6). After thermal aging at 80 °C for 7 days, this behavior is maintained, *i.e.*, all composites have comparable tensile strength values (about 40 MPa) and, as expected, all strengths are slightly lower than before thermal aging.

Table 6. Effect of dispersant and mixing conditions on the tensile properties (250 mm/s) of PVC composites before aging.

Compound	Tensile modulus (MPa)	Tensile strength (MPa)	Elongation at break (%)
<b>PVC</b>	2390	49.4	32
<b>PVC + plasticizer</b>	2032	43.2	43
PVC + plasticizer + hectorite ( <b>mo1</b> )	1920	44.9	44
PVC + plasticizer + bentonite ( <b>mo1</b> )	2230	45.7	44
PVC + plasticizer + hectorite ( <b>mo2</b> )	2172	45.0	35
PVC + plasticizer + bentonite ( <b>mo2</b> )	2037	45.2	37
<b>PVC + plasticizer + dispersant</b>	1930	42.4	75
PVC + plasticizer + dispersant + hectorite ( <b>mo1</b> )	2051	44.4	40
PVC + plasticizer + dispersant + bentonite ( <b>mo1</b> )	2243	45.5	36
PVC + plasticizer + dispersant + hectorite ( <b>mo2</b> )	2249	46.3	39
PVC + plasticizer + dispersant + bentonite ( <b>mo2</b> )	2166	45.9	27

**mo1:** mixing order 1, one-shot direct compounding.

**mo2:** mixing order 2, pre-gel of organoclay in DIDP with subsequent addition to PVC.

**Plasticizer:** di-isodecyl phthalate (DIDP, at 10 wt% loading).

**Dispersant:** propylene carbonate (at 1 wt% loading).

**Hectorite:** tallow-triethanol-ammonium modified EA-3300 (at 3 wt% loading).

**Bentonite:** tallow-triethanol-ammonium modified EA-3284 (at 3 wt% loading).

A more intriguing picture emerges when considering the effects of the plasticizer addition, order of mixing, and the presence of the dispersant on the tensile elongation at break of PVC/DIDP composites ([Table 6](#)). As expected the addition of small molecules (DIDP and dispersant) enhances the ductility of the PVC matrix. Namely, addition of 10 wt% DIDP plasticizer to PVC increases the elongation at break from about 30% to about 43% or 51%, before or after thermal aging respectively. Further addition of 1 wt% of a second small molecule (propylene carbonate dispersant) to PVC/DIDP increases the elongation at break to an even greater value of about 75%, both before and after aging. When considering the hectorite and bentonite composites, their elongation at break is maintained rather high (between 30% and 50%, independent of filler type and order of mixing) showing no marked embrittlement upon nanocomposite formation, and despite the relatively good nanofiller dispersion, which is typically accompanied by marked decreases of the composites' ductility and elongation at break<sup>[19]</sup>. The values of the composites' elongations at break are comparable to the PVC/DIDP matrix, before and after aging, and substantially lower than the 75% elongation at break of the PVC/DIDP/dispersant blend, even when dispersant is added to the composites. This effect is most probably due to the dispersant being strongly physisorbed on both clays, and thus is effectively removed from the PVC/DIDP matrix.

To generalize on the mechanical property measurements, comparing across the various formulations and processing conditions the following general trends can be identified: In the absence of all organic additives (virgin PVC matrix without any plasticizer or dispersant) the tensile moduli are improved considerably by hectorite and bentonite addition, while the tensile yield points do not change, and there is no substantial loss of the maximum elongation ([Table 5](#)). When the PVC matrix is DIDP-plasticized, composite formation with either hectorite or bentonite results again in higher tensile moduli, although the relative improvement is not as high as before, while the tensile strength and maximum elongation improve slightly ([Table 6](#)). These latter trends are seen both before and after thermal aging and are independent of the mixing order used (one-shot compounding or pre-gel). Finally, when both DIDP plasticizer and propylene carbonate dispersant are added to the PVC, composite formation with hectorite or bentonite largely cancels the effects of the dispersant on the elongation at break, as would be expected by the strong affinity of the polar ester-dispersant for the nanoclay fillers, which could function to “remove” the dispersant from the polymer matrix<sup>[20]</sup> (this argument could also account for the weak dependence of the mixing order on the tensile strength and elongation, [Table 6](#)). In general, the nanocomposites containing bentonite show a greater effect of aging on the mechanical properties than the nanocomposites containing hectorite. This mechanical reinforcement behavior (improved stiffness with no change in the yield point and no substantial embrittlement) is typical of well-designed clay nanocomposites based on stiff/high-performance polymers<sup>[19], [21], [22], [23], [24], [25]</sup>, and exceeds the performance of previous nanocomposite efforts for PVC<sup>[7], [9]</sup>. The viscoelastic, storage and loss, moduli were evaluated by dynamic mechanical analysis. This technique can be used to evaluate material stiffness at various temperatures, information which is particularly useful in the characterization of materials used in applications above room temperature. The storage modulus is plotted as function of temperature in [Fig. 1](#), and a summary of the storage modulus at 30 °C and 90 °C for each composite is shown in [Table 7](#). At 30 °C, all fillers increase the storage modulus over the unfilled PVC, with the greatest improvement shown in the composite with bentonite nanoclay (20% increase). The storage modulus is significantly lower for all the compositions at 90 °C than at 30 °C, as the PVC is now above its glass transition temperature. Again, the greatest improvement in the high temperature modulus is obtained with the bentonite-based nanoclay, followed by the hectorite-based nanoclay, with 101% and

26% increases in  $G'$  respectively over the unfilled polymer at the same temperature. The other inorganic fillers do not change markedly the storage modulus above  $T_g$ , compared to the control. Bentonite and hectorite clays have very different geometric shapes, as can be seen in the AFM pictures in Fig. 2. One can clearly see that the hectorite platelets are much smaller than those of bentonite. Consequently, different levels of mechanical reinforcement can be expected from these two nanoclays if only by virtue of their inherent geometry, even when disregarding any differences in their dispersion within the polymer matrix.

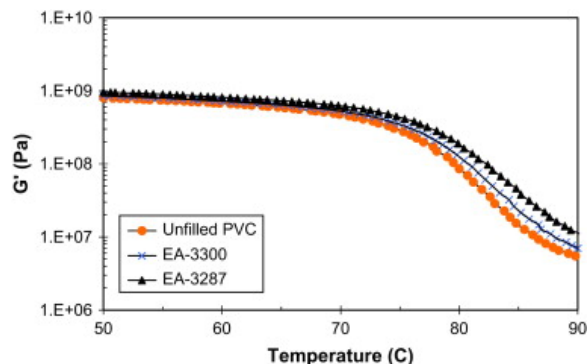


Fig. 1. Storage modulus ( $G'$ ) versus temperature for PVC composites. The composite with bentonite exhibits the largest increase in modulus particularly at temperatures above the PVC  $T_g$ .

Table 7. Storage modulus of PVC composites at 30 °C and 90 °C.

Additive type	$G'$ 30 °C (MPa)	Change <sup>a</sup> (%)	$G'$ 90 °C (MPa)	Change <sup>a</sup> (%)
No additive	899	–	5.5	–
Talc	910	1.2	5.3	–3.5
Calcium carbonate	941	4.7	6.0	9.6
Kaolin	988	9.9	6.3	13.6
Bentonite	1080	20.1	11.1	101.8
Hectorite	956	6.3	7.0	26.7

<sup>a</sup> Modulus change compared to PVC with no additive at the same temperature.

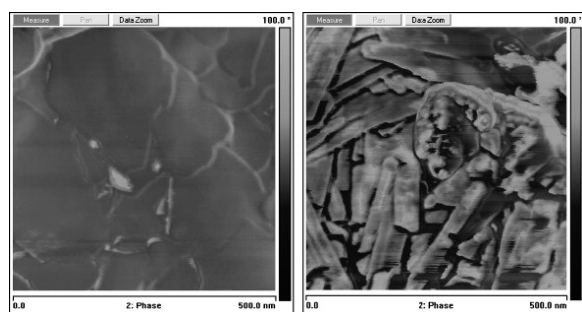


Fig. 2. AFM images of bentonite (left) and hectorite (right). The scale bar in both is 500 nm.

### 3.4. Thermal analysis

The glass transition temperature was determined using two methods, DSC and DMA. The  $T_g$  results are shown in Table 8. For all the fillers evaluated, the differences in glass transition temperature between

the composites and the unfilled PVC are not significant. The addition of these fillers has no effect on the DSC-determined  $T_g$ , indicating no significant change in the polymer thermodynamics. The DMA-determined “apparent”  $T_g$  shows the same changes with addition of clay as the storage moduli, indicating that the various clays provide similar reinforcement above and below the thermodynamic  $T_g$  (*i.e.*, a reinforcing effect of the modulus on both sides of the thermodynamic  $T_g$  would result in a shift of the  $\tan \delta$  peak towards higher temperatures and manifest in a thermomechanical (apparent)  $T_g$  change that follows the modulus change). In previous work<sup>[7]</sup>, the  $T_g$  for virgin PVC was found to be 85.3 °C, which is significantly higher than obtained in this study, and the nanocomposite formation increased the  $T_g$  by 1 or 2 °C in the same study<sup>[7]</sup>, while there is essentially no measurable effect in this study.

Table 8. Glass transition temperature of PVC composites, based on differential scanning calorimetry (DSC) and on dynamic mechanical analysis (DMA).

Additive type	$T_g$ DSC (°C)	$T_g$ DMA (°C)
No additive	77	75.9
Talc	75	74.7
Calcium carbonate	77	75.7
Kaolin	74	75.9
Bentonite	77	77.3
Hectorite	76	76.9

Thermal gravimetric analysis (TGA) has been used to comparatively evaluate the thermal decomposition of PVC and its composites, a behavior that has been shown to relate directly to the dispersion of nanoclays in a polymer matrix<sup>[26]</sup>. The key TGA results are summarized in [Table 9](#). Namely, the temperatures at weight losses of 10% ( $T_{10}$ ) and 50% ( $T_{50}$ ), and the temperature of maximum degradation ( $T_{PDR}$ , temperature at peak/maximum degradation rate) are compared, in order to evaluate the effect of filler addition on the composite thermal stability. At 10% mass loss, the nanoclays and the talc show a reduced stability compared to unfilled PVC. The composites with nanoclays show an earlier mass loss, with a significant reduction in the  $T_{10}$ . This reduction could be due to either degradation of the nanoclay organic treatment, or to an acceleration of the PVC degradation process. The  $T_{50}$  temperatures are similar for all the composites evaluated, despite the differences seen in the  $T_{10}$ , and similar to the  $T_{50}$  of the unfilled PVC. The peak degradation temperature is also not affected significantly by the fillers, maybe slightly lowered by the addition of nanoclay or talc. Thus, the addition of nanoclay appears to only accelerate the beginning of the degradation process, but does not seem to have a similar effect throughout the course of degradation. The nanoclays do not enhance the PVC's thermal stability as measured by TGA, in agreement with previous work<sup>[11]</sup>.

Table 9. Thermal stability of PVC and its composites by TGA.

Additive type	Additive level (%)	$T_{10}$ (°C)	$T_{50}$ (°C)	$T_{PDR}$ (°C)
No additive	0	282	322	290
Talc	2	278	320	287
Calcium carbonate	2	281	323	289
Kaolin	2	282	327	290
Bentonite	3 <sup>a</sup>	272	326	284
Hectorite	3 <sup>a</sup>	277	327	286

$T_{10}$  temperature at 10% weight loss.

$T_{50}$  temperature at 50% weight loss.

$T_{PDR}$  temperature at peak degradation rate.

<sup>a</sup> Bentonite and hectorite additives contain an organic modification; for both, 3 wt% additive (organo-filler) level corresponds to *ca.* 2 wt% of inorganic filler level.

### 3.5. Morphological characterization

The morphology of the clay-containing PVC systems was evaluated using a combination of X-ray diffraction (XRD) and transmission electron microscopy (TEM). Low  $2\theta$  XRD enables the evaluation of the  $d$ -spacing of the intercalated structures, by evaluating how much expansion has occurred by entry of the polymer into the gallery space of the clay. Three situations are typical: either no change in the  $d$ -spacing and the  $d_{001}$  peak of the clay is maintained, indicating no dispersion or a microcomposite structure; or a peak is observed but shifted at a lower value of  $2\theta$ , which would be a classic indication of intercalated structures in the nanocomposite; or finally, there can be either no  $d_{001}$  peak or a broad peak, an indicator of disorder (loss of parallel clay platelet stacking). In the last two cases, where some dispersion occurs, one can draw no definitive conclusion about the type of dispersion<sup>[27]</sup>, since exfoliated layers and disordered filler stacks are not detectable by XRD. The XRD traces of all of the PVC composite systems are shown in Fig. 3 and no peak is seen for any of the nanoclay-containing compounds (either bentonite or hectorite). This indicates that disorder has occurred and may denote either an exfoliated nanocomposite or a disordered microcomposite. In addition, the background at low  $2\theta$  angle is increased, especially for the composites containing both DIDP and dispersant, indicating the existence of well-dispersed fillers.

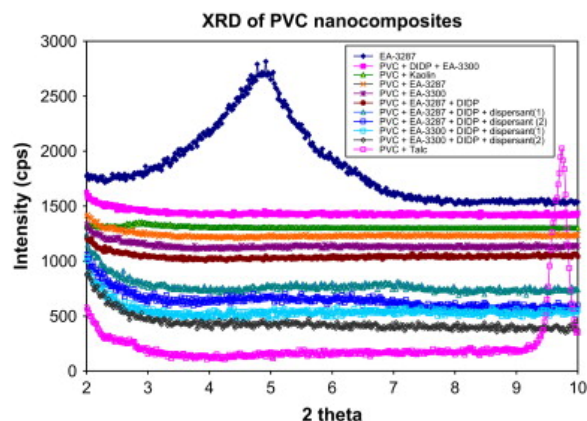


Fig. 3. XRD data for PVC with the various additives. The only systems in which a peak may be seen are that for the pristine bentonite clay (EA-3287, the top trace) and for PVC + talc (the bottom trace).

Bright field transmission electron microscopy (TEM) enables direct imaging of the clay within the polymer, and assesses filler dispersion. Despite the small areas sampled, which might not be representative of the entire structure, careful imaging at low and high magnifications, including observation of various specimens/spots, can provide a good evaluation of the composite morphology, and can be used to properly assign the composite type<sup>[27]</sup> (exfoliated, mixed-morphology nanocomposite, or disordered microcomposite). TEM images for PVC composites with both bentonite and hectorite fillers have been obtained, for the systems which do not contain additional additives and for those which contain dispersant and/or plasticizer (Fig. 4 for bentonite and Fig. 5 for hectorite). One



may conclude that both bentonite and hectorite are quite well dispersed at both the micrometer (clay agglomerates and tactoids) and at the nanometer (clay platelets) scales. In both cases, the addition of the plasticizer and dispersant promotes better dispersion of the fillers (bentonite and hectorite) in the PVC matrix. Also, both types of clays produced rather good dispersions at the nanometer scale, with individual clay platelets disorderly dispersed in the polymer with a loss of their parallel stacking. This is in very good agreement with the XRD results (Fig. 3). At the micrometer scale, bentonite shows better dispersion than hectorite. The hectorite composite shows some clustering of clay platelets in tactoids/agglomerates, ranging in size from 300 nm to 800 nm and, less-frequently, even larger agglomerates of 2–4  $\mu\text{m}$ . In all cases the structure of the composites is a mixed morphology of exfoliated and disordered nanoclay fillers, with variations in extent of dispersion from system to system.

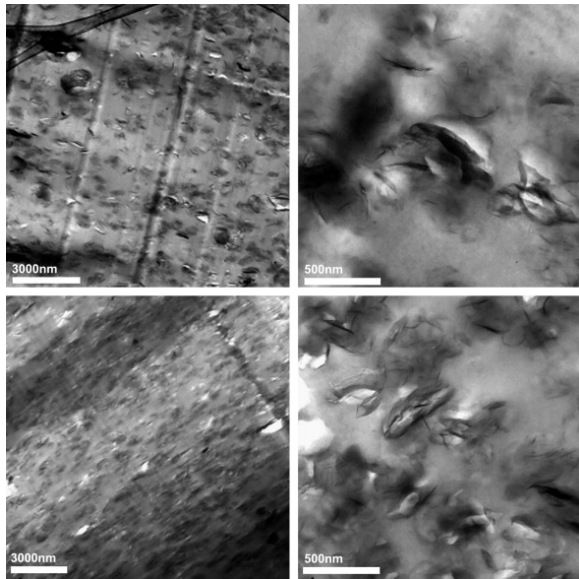


Fig. 4. The top set of images shows PVC–bentonite nanocomposites containing a dispersant while the bottom set shows the images of the nanocomposite containing only PVC and the organically-modified clay.

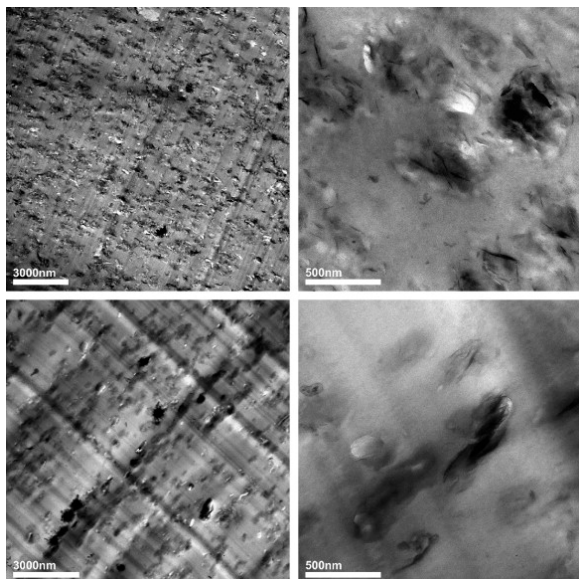




Fig. 5. The top set of images shows PVC–hectorite nanocomposites containing a dispersant while the bottom set shows the images of the nanocomposite containing only PVC and the organically-modified clay.

### 3.6. Evaluation of fire retardancy by cone calorimetry

One class of application-related testing for PVC compounds is the evaluation of fire retardancy. A well-suited laboratory technique to evaluate fire retardancy is the cone calorimeter. Parameters typically available from the cone calorimeter experiment include the heat release rate (HRR) and especially its peak value (PHRR), total heat released, volume of smoke produced (VOS), mass loss rate (MLR), time to ignition, and time to peak heat release rate. An introduction to cone calorimetry and its utility in the study of polymer–clay nanocomposites can be found in a book chapter by Schartel<sup>[28]</sup>.

In PVC applications, smoke production is usually the most important concern, and research usually is directed towards smoke suppression in PVC, rather than fire retardancy. PVC is considered to be an inherently fire retarded material due to the presence of the chlorine. The cleavage of a C–Cl bond will lead to the formation of HCl which will serve as the fire retardant<sup>[29]</sup>. The curves showing the evolution of smoke with time are provided in Fig. 6, and the smoke data is shown in Table 10. For the PVC/filler compounds, the addition of talc, kaolin, plasticizer or quaternary ammonium organic modifier (Fig. 6a and b) has little effect on the course of smoke evolution, although an increase in the total volume of smoke is seen upon addition of talc or the organic modifier. When a clay is added to unplasticized PVC, the smoke evolution is significantly reduced, especially for bentonite (Fig. 6c). For the PVC/DIDP compounds a reduction in volume of smoke is seen for all the formulations, with the greater reduction seen with bentonite organoclay (Fig. 6d).

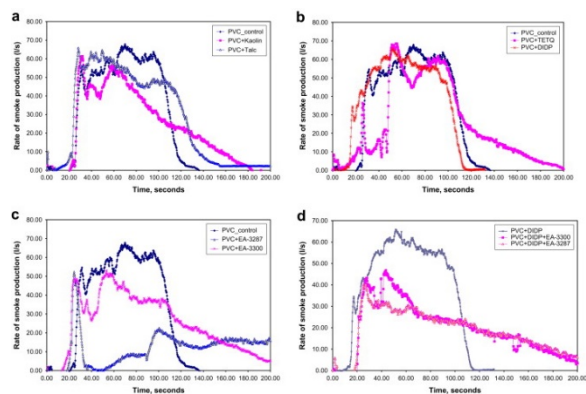


Fig. 6. Smoke evolution curves for PVC and combinations with the various additives. (a) PVC and PVC with talc and kaolin and shows no change in smoke evolution. (b) The addition of neither the organic modification nor the plasticizer has an effect on smoke evolution. (c) The addition of either bentonite (EA-3287) or hectorite (EA-3300) lowers the amount of smoke with bentonite showing a lower value and (d) shows that in plasticized PVC, the addition of either clay reduces the smoke.

Table 10. Smoke, heat release and mass loss cone calorimetry data for PVC and its composites at 50 kW/m<sup>2</sup>.

Compound	VOS (L)	$\Delta_{VOS}$ (%)	PHRR (kW/m <sup>2</sup> )	$\Delta_{PHRR}$ (%)	THR (MJ/m <sup>2</sup> )	AMLR (g/s m <sup>2</sup> )	$\Delta_{AMLR}$ (%)
PVC	10.0	0	70	0	1000	1.0	0
PVC+Kaolin	11.0	10	70	0	1000	1.0	0
PVC+talc	12.0	20	70	0	1000	1.0	0
PVC+DIDP	9.0	-10	70	0	1000	1.0	0
PVC+DIDP+EA-3300	8.0	-20	70	0	1000	1.0	0
PVC+DIDP+EA-3287	7.0	-30	70	0	1000	1.0	0
PVC+EA-3287	6.0	-40	70	0	1000	1.0	0
PVC+EA-3300	5.0	-50	70	0	1000	1.0	0

<b>PVC</b>	4711 ± 6 6	NA	336 ± 1 2	NA	32 ± 1	37 ± 3	NA
PVC + kaolin	4403 ± 7 1	7	277 ± 4	18	32 ± 1	22 ± 1	41
PVC + bentonite	2992 ± 3 70	36	233 ± 1 1	31	32 ± 2	16 ± 2	57
PVC + hectorite	4066 ± 1 50	14	293 ± 1 1	13	34 ± 1	20 ± 2	46
PVC + organic modifier	4916 ± 2 7	0	341 ± 1 8	0	33 ± 1	25 ± 1	32
PVC + talc	5004 ± 2 55	0	310 ± 3	8	31 ± 0	29 ± 1	22
<b>PVC + DIDP</b>	4531 ± 2 57	NA	397 ± 4	NA	35 ± 0	38 ± 3	NA
PVC + DIDP + hectorite	3516 ± 2 74	22	310 ± 8	8	38 ± 1	19 ± 2	53
PVC + DIDP + bentonite	3366 ± 5 76	26	287 ± 8	15	37 ± 1	18 ± 0	53
PVC + DIDP + dispersant	4726 ± 2 17	0	345 ± 2 3	0	36 ± 1	32 ± 3	16
PVC + DIDP + dispersant + bentonite ( <b>mo1</b> )	3265 ± 3 5	28	285 ± 1 7	15	38 ± 1	17 ± 1	55
PVC + DIDP + dispersant + bentonite ( <b>mo2</b> )	3698 ± 6 2	18	276 ± 9	18	39 ± 1	16 ± 1	58
PVC + DIDP + dispersant + hectorite ( <b>mo1</b> )	4302 ± 1 51	5	301 ± 9	10	38 ± 1	19 ± 2	50
PVC + DIDP + dispersant + hectorite ( <b>mo2</b> )	3992 ± 2 1	12	276 ± 4	18	39 ± 0	15 ± 1	61

PHRR, peak heat release rate; THR, total heat released; VOS, volume of smoke produced during combustion; AMLR, average mass loss rate;  $\Delta_x$ , percent **reduction** in property X compared to virgin PVC or to unfilled PVC + DIDP; DIDP, plasticizer.

Considerable smoke reduction is observed for all PVC–nanoclay composites as compared to the unfilled PVC control. An unprecedented and significant decrease in smoke production is thus obtained using only low filler content. The total evolved volume of smoke decreases, and smoke is evolved at lower amounts over a longer period of time. On the other hand, the smoke evolution for the nanocomposites begins earlier than for the PVC containing other inorganic fillers. This observation appears to be in agreement with the TGA mass loss results reported above, in which the addition of nanoclay reduces  $T_{10}$ , but not  $T_{50}$ . The mixing order and the type of nanoclay (bentonite or hectorite) does not have a significant effect on the volume of smoke produced.

This smoke data must be compared to the data on thermal degradation. With PVC, the degradation pathway leads to the loss of HCl, which gives conjugated double bonds. These bonds will eventually cyclize to form aromatic compounds which give the smoke. Thus a decreased thermal stability means increased HCl evolution and should lead to an increased production of aromatics and hence more

smoke. The amount of the organic modifier is around 1% of the total sample so it is very unlikely that this small amount of material could have a pronounced effect on the total sample, nonetheless, since this is frequently cited as one of the possible reasons for an earlier time to ignition for polymer–clay nanocomposites, it cannot be completely eliminated from consideration. One can see that the cone calorimetric data do not agree with this assessment. There can be no doubt that the addition of the clay leads to more HCl evolution and so the combination of this with the cone calorimetric data suggests that perhaps one can unlink the formation of aromatics from the loss of HCl. This could be due to some effect of the clay leading to a decreased production of aromatics. This requires further investigation.

The effect of an organically-modified montmorillonite on smoke production is quite variable – there is no certain trend where one can say that smoke is always increased or decreased. The data in a paper on some polystyrene nanocomposites using a few different organic modifications<sup>[30]</sup> shows that in some cases there is an increase in smoke and in others the smoke decreases by a little. The reductions in smoke in this work are unprecedented and indicative of an unusual process which is occurring.

The smoke, peak and total heat release and mass loss cone calorimetric data are presented in [Table 10](#), and the time to ignition and time to PHRR are shown in [Table 11](#). The addition of an inorganic material, whether hectorite, bentonite, talc or kaolin, brings about a reduction in the peak heat release rate. Based on previous work on nanocomposites<sup>[31]</sup>, one expects that the addition of clay will decrease the PHRR and that this occurs because the mass loss decreases. As can be seen in this table, for all formulations there is a much larger reduction in the mass loss rate than in the PHRR, which implies that this system is different in some ways from other polymers. When either the organic modifier only or the plasticizer only are added to PVC, the PHRR increases since this increases the fire load. Indeed, in systems which contain the plasticizer, in addition to other entities, a decrease in the time to ignition is seen ([Table 11](#)).

Table 11. Time to ignition and time to PHRR cone calorimetry data for PVC and its composites at 50 kW/m<sup>2</sup>.

Compound	$t_{ig}$ (s)	$t_{PHRR}$ (s)
<b>PVC</b>	25 ± 1	51 ± 14
PVC + kaolin	25 ± 3	34 ± 2
PVC + bentonite	21 ± 1	28 ± 1
PVC + hectorite	20 ± 1	43 ± 13
PVC + organic modifier	24 ± 2	61 ± 5
PVC + talc	24 ± 1	33 ± 1
<b>PVC + plasticizer</b>	16 ± 3	58 ± 6
PVC + plasticizer + bentonite	18 ± 1	26 ± 0
PVC + plasticizer + hectorite	19 ± 1	37 ± 5
<b>PVC + plasticizer + dispersant</b>	18 ± 1	42 ± 4
PVC + plasticizer + bentonite + dispersant ( <b>mo1</b> )	18 ± 2	25 ± 1
PVC + plasticizer + bentonite + dispersant ( <b>mo2</b> )	19 ± 1	24 ± 2
PVC + plasticizer + hectorite + dispersant ( <b>mo1</b> )	18 ± 1	29 ± 2
PVC + plasticizer + hectorite + dispersant ( <b>mo2</b> )	17 ± 2	26 ± 2

$t_{ig}$ , time to ignition;  $t_{PHRR}$ , time to PHRR; plasticizer, di-isodecyl phthalate (DIDP, at 10 wt% loading).

Another important parameter that is evaluated by the cone calorimeter is the heat release rate curve, and these are shown in [Fig. 7](#). The addition of a clay to the uncompounded PVC, whether hectorite, bentonite, talc or kaolin, leads to a decreased intensity in the heat release rate curve ([Fig. 7a](#)), no change in the total heat released and there is minimal change in the time to ignition. When plasticizer only is added, the time to ignition is shortened and the PHRR is increased, since there is an increased fuel load. The heat release rate curves for plasticized PVC ([Fig. 7b](#)) show a lower peak of heat release than in unplasticized PVC and there is a little difference between hectorite and bentonite clays.

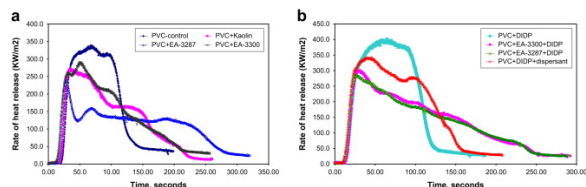


Fig. 7. Heat release rate plots for PVC and combinations. (a) The curves on unplasticized PVC while (b) for plasticized PVC.

## 4. Conclusions

PVC compounds, formulated with various additives, are versatile plastics that find applications in a variety of industries. Hence, PVC is one of the most widely used thermoplastic polymers today. This useful polymer does, however, degrade readily during processing and this has been a limiting problem when formulating nanoclay PVC composites. Careful selection of a suitable nanoclay organic modifier allows for the successful preparation of such composites. We formulated various nanoclay PVC composites using a simple melt blending approach. Careful analysis showed that the nanoclay is well dispersed in the PVC compound both at the micro- and nano-scale levels. The excellent nanoclay dispersion leads to significantly enhanced mechanical properties, notably an increase in modulus with no significant loss of either tensile strength or elongation. The blend of properties that have been observed for the PVC nanocomposites reported herein suggests that this is the first true PVC nanocomposite and an area for future research.

PVC composite thermal stability, as measured by a classic HCl evolution method specific for PVC, is somewhat lowered for the nanoclay composites as compared to appropriate control formulations. Another assessment of composite thermal stability by thermogravimetric analysis shows that the nanoclay affects the degradation mechanism of the PVC. The temperature where a 10% mass loss of the composite is registered is slightly decreased, but the temperature where a 50% mass loss occurs is slightly increased as compared to the unfilled PVC.

One may anticipate further developments in PVC nanocomposites involving other less-basic amines, imidazolium-based materials come immediately to mind, used with a montmorillonite-type clay, or layered double hydroxides, in which the hydroxides may be able to absorb the HCl as it evolves. The price of the imidazolium-based surfactants makes this unlikely to be successful for PVC on a commercial scale. For the layered double hydroxides, there are significant problems in obtaining well-dispersed LDHs in many polymers which must be overcome before this can be a practical solution to PVC nanocomposites.

PVC composites that contain well-dispersed nanoclay show a significant decrease in smoke production. This finding of smoke reduction is not in agreement with the classic measurement of thermal stability,

and thus suggests that the assumed mechanism of smoke generation during burning, of HCl loss leading to the formation of aromatic species, may need revision. Regardless of the degradation model, the fact that nanoclay can suppress smoke generation is of great importance for numerous PVC applications where smoke suppression is of concern. Examples of applications include, among others, wire and cable, and foamed insulation.

## Appendix. Supplementary data

<https://ars.els-cdn.com/content/image/1-s2.0-S0032386109001244-mmc1.doc>

## References

- [1] Gilman JW, Awad W, Davis RD, Shields J, Harris Jr RH, Davis C, et al. *Chem Mater* 2002;14:3776–85.
- [2] Costache MC, Heidecker MJ, Manias E, Gupta RK, Wilkie CA. *Polym Degrad Stab* 2007;92:1753–62.
- [3] Liu J, Chen G, Yang J. *Polymer* 2008;49:3912–27.
- [4] Wang D, Parlow D, Yao Q, Wilke CA. *J Vinyl Addit Technol* 2001;7:203–13.
- [5] Wang D, Parlow D, Yao Q, Wilke CA. *J Vinyl Addit Technol* 2002;8:139–50.
- [6] Yalcin B, Cakmak. *Polymer* 2004;45:6623–38.
- [7] Wan C, Zhang Y, Zhang Y. *Polym Test* 2004;23:299–306.
- [8] Zanetti M, Valesella S, Luda MP, Costa L. Fire and polymers IV. Materials and concepts for hazard prevention. In: Wilkie CA, Nelson GL, editors. ACS symposium series 922; 2006. p. 75–88.
- [9] Chen C-H, Teng C-C, Tang C-H. *J Polym Sci Part B Polym Phys* 2005;43: 1465–74.
- [10] Peprnicek T, Duchet J, Kovarova L, Malac J, Gerard JF, Simonik J. *Polym Degrad Stab* 2006;91:1855–60.
- [11] Francis N, Schmidt D. The toxics use reduction Institute University research in sustainable technologies program; 2006; Francis N, Schmidt D. PVC/layered silicate nanocomposites: preparation, characterization, and properties, ANTEC; 2007.
- [12] Beyer G. *J Fire Sci* 2007;25:65–78; Beyer G. *Polym Adv Technol* 2008;19:485–8.
- [13] Matuana LM, Faruk O. ANTEC 2007:1243–7.
- [14] Wang D, Wilkie CA. *J Vinyl Addit Technol* 2002;8:238–45.
- [15] Gong F, Feng M, Zhao C, Zhang S, Yang M. *Polym Degrad Stab* 2004;84: 289–94.
- [16] Du J, Wang D, Wilkie CA, Wang J. *Polym Degrad Stab* 2003;79:319–24.
- [17] Cullis CF, Hirschler MM. The combustion of organic polymers. Oxford: Clarendon Press; 1981. p. 117, 143–6.
- [18] Elementis rheology handbook, Elementis Specialties; 2008.
- [19] Alexandre M, Dubois P. *Mater Sci Eng R* 2000;28:1; Mai Y, Yu Z, editors. Polymer nanocomposites. Woodhead Publishing; 2006.
- [20] Manias E. *Nat Mater* 2007;6:9–11; Kuppa V, Manias E. *Eur Phys J E* 2002;8:193–9; Manias E, Subbotin A, Hadziioannou G, ten Brinke G. *Mol Phys* 1995;85: 1017–32.
- [21] Strawhecker KE, Manias E. *Chem Mater* 2000;12:2943–9; Strawhecker KE, Manias E. *Macromolecules* 2001;34:8475–82.
- [22] Manias E, Touny A, Wu L, Strawhecker K, Lu B, Chung TC. *Chem Mater* 2001;13:3516–23.
- [23] Wang ZM, Chung TC, Gilman JW, Manias E. *J Polym Sci B Polym Phys* 2003;41:3173–87.
- [24] Sinha Ray S, Okamoto M. *Prog Polym Sci* 2003;28:1539; Pinnavaia TJ, Beall GW, editors. Polymer–clay nanocomposites. West Sussex: Wiley; 2000; Giannelis EP, Krishnamoorti R, Manias E. *Adv Polym Sci* 1999;138:107–47.

- [25] Zhang J, Manias E, Wilkie CA. *J Nanosci Nanotechnol* 2008;8:1597–615.
- [26] Constance MC, Heidecker MJ, Manias E, Wilkie CA. *Polym Adv Technol* 2006;17:764–71; Constance MC, Wang D, Heidecker MJ, Manias E, Wilkie CA. *Polym Adv Technol* 2006;17:272–80; Costache MC, Heidecker MJ, Manias E, Camino G, Frache A, Beyer G, et al. *Polymer* 2007;48:6532–45.
- [27] Morgan AB, Gilman JW. *J Appl Polym Sci* 2002;87:1329–38.
- [28] Schartel B. In: Morgan AB, Wilkie CA, editors. *Flame retardant polymer nanocomposites*. New York: John Wiley & Sons; 2007. p. 107–30.
- [29] Georgette P, Simons J, Costa L. In: Grand AF, Wilkie CA, editors. *Fire retardancy of polymeric materials*. New York: Marcel Dekker; 2000. p. 245–84.
- [30] Zhu J, Morgan AB, Lamelas FJ, Wilkie CA. *Chem Mater* 2001;13:3774–80.
- [31] Gilman JW, Jackson CL, Morgan AB, Harris Jr R, Manias E, Gianellis EP, et al. *Chem Mater* 2000;12:1866–73.